CHAPTER

17

Optogenetic Intracranial Self-Stimulation as a Method to Study the Plasticity-Inducing Effects of Dopamine

Michael T. Lippert[*,§,1], *Kentaroh Takagaki*[*,¶], *Theresa Weidner*[*], *Marta Brocka*[*], *Jennifer Tegtmeier*[*], *Frank W. Ohl*[*,§,¶]

[*]Department Systems Physiology of Learning, Leibniz Institute for Neurobiology, Magdeburg, Germany; [§]Center for Behavioral Brain Sciences (CBBS), Otto-von-Guericke-University Magdeburg, Magdeburg, Germany; [¶]Institute of Biology, Otto-von-Guericke-University Magdeburg, Magdeburg, Germany

[1]Corresponding author

1. INTRODUCTION

1.1 Research Perspective

The observation that brain stimulation can motivate learning and may have appetitive properties dates back to the origins of modern neuroscience (Delgado et al., 1954; Olds and Milner, 1954). Stimulation of several nuclei in the brain stem is appetitive enough to sustain self-stimulation in animals. In particular, the lateral hypothalamic area (LHA) was found early on to support self-stimulation (Olds and Milner, 1954). While the precise anatomy of the midbrain was not fully understood at the time, it was gradually learned that the ventral tegmentum and the medial forebrain bundle (MFB) are the essential structures supporting such self-stimulation; for example, lesions to these structures reduce or abolish self-stimulation behavior in response to electrical stimulation of the LHA (Boyd and Gardner, 1967; Olds and Olds, 1969). Subsequent decades of research revealed that mesolimbic dopaminergic projections from the ventral tegmental area (VTA) to the nucleus accumbens (NAcc) within the MFB are also critical for many other types of self-stimulation, and substance self-administration behavior (Stuber and Wise, 2016).

Signals conveyed by the mesolimbic dopamine system are related in particular to reward prediction error (Schultz, 2017; Steinberg et al., 2013). Reward prediction error is an elementary signal postulated in various theories of learning to allow adaptation of behavior to maximize external reward. For example, reward prediction error explains classical conditioning through the Rescorla–Wagner model (Rescorla and Wagner, 1972), where it determines magnitude and direction of changes in the model over time. In the brain, dopamine release by the mesolimbic dopamine system can signal the difference between expected and obtained reward and therefore allows the organism to change synaptic weights through plasticity, thereby adapting its behavior to maximize obtained reward. As such, it is a key signal for fundamental survival mechanisms.

Traditionally, electrical stimulation of either the MFB or VTA has been used to study the function of the mesolimbic dopamine system. In addition to the study of the circuit-level functioning of this brain reward system, the technique has also become a valuable tool in addiction research (Negus and Miller, 2014; Vlachou and Markou, 2011). However, because dopamine—through prediction error signaling—has a strong influence on neural plasticity, electrical midbrain stimulation has also been instrumental in documenting this influence on plasticity (Bao et al., 2001; Kadar et al., 2011; Reichenbach et al., 2015). While electrical stimulation offers a more direct link to translational research and is technically less challenging, in terms of mechanistic research, it has the disadvantage of lacking cellular selectivity. For example, the VTA is

Handbook of In Vivo Neural Plasticity Techniques
https://doi.org/10.1016/B978-0-12-812028-6.00017-3

composed of different cell types that are not exclusively dopaminergic (Morales and Margolis, 2017). In case of the MFB, cell-type heterogeneity is even greater, with virtually all brain stem neuromodulatory systems represented (Harvey et al., 1963; Takagi et al., 1980). Stimulating these structures therefore results in the release of a variety of transmitters from various cell types, which modify the effects of dopamine and dopaminergic cells. The recent development of optogenetics has allowed selective stimulation of specific cell types. By introducing opsins, which are light-sensitive proteins commonly found in algae, fungi, and archaea, genetically defined populations of cells can be made light sensitive (Boyden et al., 2005; Deisseroth, 2015). Soon after the invention of the technique, it was adapted to study the effects of dopaminergic cell stimulation (Tsai et al., 2009). For example, in a seminal paper, the relationship between mesolimbic dopamine release and prediction error was concisely demonstrated (Steinberg et al., 2013). This achievement critically hinged on the ability to control the mesolimbic dopamine system with sufficient cell-type specificity.

Mesolimbic dopamine system stimulation with optogenetics has been used in neuroplasticity research on two levels: research into dopamine-related circuit dynamics and research into dopamine-related modulations of behavior.

In terms of dopamine-related circuit dynamics, it can be used to study the basic circuit functionality of the various projections of the mesolimbic dopamine system (Adamantidis et al., 2011; Tsai et al., 2009). For example, the VTA sends its main projections to the striatum, particularly the NAcc, as well as to prominent cortical target areas such as the prefrontal cortex. Here, optogenetic stimulation can be used to investigate how release of dopamine plastically reshapes circuits (Ellwood et al., 2017; Morales and Margolis, 2017). In addition to these main projections, further projections terminate in sensory cortices (Budinger et al., 2008; Lou et al., 2014; Mylius et al., 2015; Schicknick et al., 2008), and these sparse projections seem to play a key functional role in cortical plasticity. This is underscored, for example, by the dopamine sensitivity of auditory cortex–dependent learning (Schicknick et al., 2008; Stark and Scheich, 1997). Use of optogenetic VTA stimulation is therefore a valuable tool to investigate the function of these cortical projection systems and their plastic changes.

In terms of research into dopamine-related modulations of behavior, optogenetic VTA stimulation can be used as a brain stimulation reward in learning experiments, because the strong appetitive effects of the stimulation permit its direct use as a reinforcing stimulus (Shumake et al., 2010). In such paradigms, stimulation of a known neural circuit is used to substitute for natural external reward. Natural external reward is associated with the widespread activation of additional neuronal circuits that are not directly associated with reward processing, but instead are related to behavioral cue/operant processing, such as somatosensation or gustatory processing. In addition, external reward timing is often difficult to control precisely, or can only be administered at certain delayed time-points within behavioral trials. Using brain stimulation reward bypasses these limitations and allows the application of a direct and immediate reinforcement. Furthermore, optogenetic brain stimulation reward can be finely titrated in terms of appetitive strength, which is difficult with natural external rewards such as food reinforcement. Such fine titrations of appetitive strength allow it to be employed to better understand the role of the dopaminergic system in addiction (Hjelmstad et al., 2013; Langlois and Nugent, 2017).

1.2 Optogenetic Ventral Tegmental Area Stimulation in Rodents: Passive Stimulation and Intracranial Self-Stimulation

1.2.1 Inherent Advantages of Optogenetic Ventral Tegmental Area Stimulation

Optogenetic stimulation offers a powerful method to selectively stimulate dopaminergic neurons in the VTA with a clear functional read-out provided by self-stimulation behavior. In contrast to electrical stimulation of the VTA or MFB, optogenetic stimulation offers enhanced cell-type specificity (Deisseroth, 2015; Witten et al., 2011) by the very nature of genetic targeting.

In addition to genetic specificity, optogenetic stimulation is also spatially localized because the spread of the typically used blue or green light is very limited in brain tissue (Al-Juboori et al., 2013; Yona et al., 2016). This spatial selectivity of optogenetic stimulation surpasses what can be achieved with electrical or pharmacogenetic methods. For example, electrical stimulation has a large radius of action, and because dopaminergic cells in the VTA and substantia nigra (SN) are located in immediate spatial proximity, the large range of action can be problematic. The effective range of electrical stimulation is strongly dependent on the size of neural elements (Ranck, 1975), and as a result, undesired stimulation of small passing fibers may occur at intensities required to stimulate the intended targets, the larger VTA cell bodies. In the case of pharmacogenetic methods, genetic cell-type specificity can be achieved, but spatial selectivity is limited due to diffusion—both diffusion of the pharmacogenetic designer drug and of the genetically targeted viral vector. This lack of spatial selectivity is particularly problematic as the VTA and *substantia nigra pars compacta* (SNc) cells share common functions, and activation of either structure is sufficient to induce self-stimulation. Only by combining the genetic and spatial specificity of optogenetic stimulation can one dissociate

between the functions of these two regions (Ilango et al., 2014b).

In principle, advanced strategies targeting multiple genes can be used to dissociate the VTA from SNc (Fenno et al., 2014). However, these strategies are technically more challenging. Especially for optogenetic VTA stimulation in rodents, a single recombinase system in combination with anatomically precise fiber placement offers a favorable trade-off between stimulation specificity and technical robustness. An alternative approach to anatomically specific targeting of VTA circuits with optogenetics is to stimulate terminal fibers originating from the VTA, resulting in dopamine release within a structure of interest, e.g., auditory cortex (Tye and Deisseroth, 2012). This approach achieves a more spatially precise release, but has a number of key drawbacks that must be considered. First and foremost, optogenetic stimulation of terminals can generate backpropagating action potentials. These action potentials can secondarily activate additional projections of the particular cell. In this case, global dopamine release in other projection targets of a cell can result, with no simple way to assess the extent of this effect. Direct somatic stimulation in the VTA does indeed cause release in the various projection regions, yet these effects are predictable and can be considered during planning of the experiment: local application of dopamine receptor antagonists, for example, can confirm the localization of a particular effect.

An important advantage of direct VTA stimulation, in comparison with projection-specific stimulation, is the highly appetitive nature of this type of stimulation, which allows it to serve as a robust behavioral test of stimulation functionality in subsequent intracranial self-stimulation experiments. Terminal stimulation is often not strongly appetitive, precluding use of such functional read-outs (Ellwood et al., 2017). For such terminal stimulation, one can only use indirect read-outs of the effects, in conjunction with a separate effect which is secondarily affected, for example, memory. Such read-out is indirect and delayed and is therefore not suitable to immediately assess whether stimulation is successful. There are many reasons for stimulation failure, including insufficient opsin expression, insufficient light penetration, and thermal damage (Arias-Gil et al., 2016)—such pernicious problems can only be easily ruled out if one is directly stimulating the VTA and monitoring a direct, integrative behavioral read-out.

1.2.2 *Inherent Limitations of Optogenetic Ventral Tegmental Area Stimulation*

As with any scientific method, the method described here has its limitations. In general, the latter can be divided into limitations arising from optogenetic stimulation and limitations arising from VTA stimulation itself.

With regard to optogenetic limitations, as described in the introduction, the stimulation of the VTA itself can be problematic. As mentioned already, the connections of the VTA are highly diverse. As a result, many areas of the brain receive dopaminergic input. This input has been demonstrated to lead to significant plasticity in areas not immediately associated with dopamine release (Decot et al., 2017). The influence in direct projection targets such as the dorsal striatum, NAcc, and prefrontal cortex may even be more effective and may even feature some characteristics of addiction-like states (Cooper et al., 2017; Singer et al., 2017). Even low levels of stimulation may potentially lead to widespread synaptic changes. This limitation of optogenetic VTA stimulation can partially be circumvented by projection-specific stimulation. However, this often prohibits the use of self-stimulation to confirm stimulation success and may lead to unintended stimulation of remote areas through backpropagating action potentials. In addition, the evoked effect might not be strong enough to be behaviorally observable because often only a limited number of terminals are stimulated in the target region due to limited light penetration.

A second limitation of the technique described here is its limited ability to reliably discern the different substructures of the VTA (Morales and Margolis, 2017). We have noted during our experiments that stimulating the posterior part of the VTA resulted in more pronounced self-stimulation. However, because tyrosine hydroxylase (TH-Cre) or dopamine transporter (DAT-Cre) lines do not allow selectively targeting subnuclei of the VTA, such observations remain anecdotal at the moment. Improved molecular tools or projection-specific investigations, for example, using novel retrograde tracers (Cardozo Pinto and Lammel, 2017; Tervo et al., 2016) are likely to improve our understanding of the contributions of different subnuclei in the future. Interestingly, adeno-associated viruses (AAVs) have been demonstrated to show retrograde labeling even in commonly used serotypes (Aschauer et al., 2013). This could already lead to unintended stimulation effects if terminals of upstream areas are stimulated and, for example, norepinephrine is released in the VTA.

One commonly overlooked limitation of optogenetic stimulation is that expression of foreign proteins interferes with normal cell function. For example, the better expression of an exogenous protein is, the more metabolic load is applied to a cell, providing negative selective pressure and a less favorable cellular energy state (Glick, 1995). Strong firing elicited by optogenetics can also lead to metabolic burden. Furthermore, expressing channelrhodopsin 2 (ChR2) under an exogenous TH-promoter *per se* can decrease endogenous TH

enzyme expression, resulting in changes in the intrinsic function of the stimulated neurons. If expression becomes even stronger, cells can even be lost. To minimize the negative effects of this issue, expression levels and the behavior of the animal should be monitored and the experiment performed within the shortest possible time frame. However, due to the viral infection cycle of AAVs, 2 or 3 weeks of expression time must be planned. If stimulation starts too early, changes in self-stimulation behavior may predominantly reflect increasing opsin concentration in the cells and would be less informative as to plasticity or other processes of interest. A time delay of weeks between surgery and the behavioral experiment is inherent to optogenetics and slows optogenetic experiments compared with, for example, electrical stimulation experiments.

Furthermore, while optical stimulation hardware can be manufactured 'in house' to some degree, the method is significantly more expensive and difficult compared with electrical or pharmacological stimulation. Because of various safety concerns and the novelty of the technique, the clinical utility of optogenetics is inherently limited. It is therefore difficult to extrapolate results from selective optogenetic VTA stimulation in rodent models to humans, where only less selective electrical stimulation has been used (Akram et al., 2016). Research into this relationship between optogenetic and electrical stimulation is therefore of great importance, should future clinical applications of optogenetics be considered.

A further limitation of optogenetic VTA stimulation concerns the intracranial self-stimulation procedure described here. Such self-stimulation can be either used to confirm the correct placement of the fiber in the VTA or to induce neural plasticity by repeated dopamine release. However, for optogenetic self-stimulation we have observed an apparently lower magnitude of induced brain stimulation reward and a change in this magnitude over time when compared with electrical stimulation. For electrical stimulation, pressing rates quickly reach the level determined by the respective stimulation parameters in each animal. This property has made it very useful in self-stimulation experiments to assess the rewarding effects of drugs using the curve-shift method (Negus and Miller, 2014). For purely optogenetic stimulation in Cre animals, however, we have instead observed a gradual increase in press rates over many days, which appear to be less rapid than what is typically found for electrical stimulation (Fig. 17.3). The time course of this process resembles a learning curve, and press rates stabilize only after several days of repeated self-stimulation. Whether this effect is due to optogenetic stimulation affecting a smaller tissue volume, or due to additional transmitters that are released by electrical stimulation, remains to be investigated.

2. METHODS FOR OPTOGENETIC VENTRAL TEGMENTAL AREA STIMULATION AND INTRACRANIAL SELF-STIMULATION

2.1 Choosing an Animal Model

Optogenetic VTA stimulation is possible in all common laboratory rodent models. We have previously used it in mice, rats, and gerbils (Helbing et al., 2016; Kolodziej et al., 2014). However, convenient genetic targeting with dopaminergic Cre-driver lines is currently only possible in mice and rats. Promoter-driven approaches of genetic targeting are feasible for all rodent models.

In rats, the most commonly used strain for Cre-lox-driven genetic targeting is LE-Tg(TH-Cre)3.1Deis (Decot et al., 2017; Steinberg et al., 2013; Witten et al., 2011). This strain expresses Cre recombinase in tyrosine hydroxylase−positive cells. The expression specificity for dopaminergic cells, as defined by the presence of tyrosine hydroxylase in the VTA, is close to 100%. In addition, in areas outside the VTA, the strain can also be used to target noradrenergic cells, which is a potential benefit over other dopamine-targeted strains such as DAT-Cre rats which express Cre recombinase under the dopamine transporter (DAT) promoter. Such additional dopamine-targeting strains are available commercially and academically for both the TH promoter and DAT promoter and are available, for example, from Horizon Discovery, SAGE Labs, or the National Institute on Drug Abuse (NIDA). LE-Tg(TH-Cre)3.1Deis as well as a DAT-Cre line LE-Tg(DAT-iCre)6Ottc from NIDA is available for academic research on a per-cost basis and can be bred freely. However, these academic strains are based on Long−Evans rats, and commercial lines may be advantageous if a Sprague Dawley background is preferred. If no transgenic line can be used, a standard promoter-targeted viral transduction strategy is an alternative. AAV vectors are typically used for this purpose but have a limited payload capacity which does not allow inclusion of a full TH- or DAT promoter into the optogenetic construct. As a result, cell-type specificity for dopaminergic cells is diminished. We have had positive experiences with (calcium calmodulin kinase IIα (CaMKIIα)) constructs in AAV vectors applied to the VTA. These constructs generally lead to strong expression of ChR2 in mostly dopaminergic VTA cells and result in self-stimulation behavior which is indistinguishable from animals stimulated through recombinase-based ChR2 expression. Although CaMKIIα is not *per se* specific for dopaminergic neurons, targeting opsin expression with this promotor does allow one to circumvent expression in the numerous VTA inhibitory cells. This approach does not dissociate

between glutamatergic and dopaminergic cells; it nonetheless provides significantly more specificity over other methods such as electrical stimulation.

In mice too, both recombinase and promoter-targeted viral approaches are possible. While TH-Cre mouse lines were initially used for optogenetic VTA stimulation in mice (Ilango et al., 2014a), it has been shown that popular lines have a somewhat high level of ectopic expression, and the use of DAT-Cre mice has become more widespread (Morales and Margolis, 2017). In particular, the B6.SJL-Slc6a3tm1.1(Cre)Bkmn/J strain has been demonstrated to be highly selective for dopaminergic cells (Lammel et al., 2015). If a TH-Cre line is still preferred, B6.Cg-Tg(TH-Cre)1Tmd/J mice can be used, as they show a relatively dopamine-specific expression, albeit less than the above mentioned DAT-Cre line (Lammel et al., 2015). One disadvantage of the DAT-Cre line mentioned earlier, which may justify the use of a TH-Cre line instead, is that these mice are reported to have reduced DAT protein levels in the striatum (Bäckman et al., 2006). Mutations in the DAT gene have been associated with antisocial personality traits in humans (Cherepkova et al., 2016), and we have also observed altered behavioral traits in DAT-Cre mice, particularly increased aggressiveness. If no transgenic mouse line can be used, again, the use of CaMKIIα-driven opsin expression is a viable alternative (Kolodziej et al., 2014).

In contrast to mice and rats, TH- and DAT-Cre lines have yet to be established in alternative rodent models such as Mongolian gerbils. Hence, the only available option for optogenetic VTA stimulation in alternative rodents at the moment is a promoter-driven approach, for example, using the CaMKIIα promoter. In our experiments, we have found this approach to elicit robust self-stimulation in gerbils. Nonetheless, the caveats regarding promoter specificity described earlier for rats also apply here.

2.2 Choosing an Opsin Construct and Vector

Apart from the selection of a suitable animal species, strain, and targeting strategy, the actual opsin must be selected and applied to the target region.

The most commonly used opsin is ChR2(H134R), a mutated channelrhodopsin which passes higher currents compared with wild-type ChR2 (Lin, 2011). It has its absorption peak in the blue range, necessitating the use of a blue laser (typically with a wavelength of 473 nm). In rats, mice, and gerbils, we found it to be a suitable choice for optogenetic VTA stimulation. However, under some circumstances, especially in rats and gerbils, the use of a longer wavelength opsin might be preferred because longer wavelengths allow a larger tissue volume to be stimulated due to less scattering. A suitable candidate for such an opsin would be the opsin chimera C1V1, which we have successfully used in the E162T variant. This opsin can be stimulated with a green laser, which is considerably more affordable than blue lasers with equal power output. Red lasers in combination with a red light−sensitive opsin allow the highest possible penetration depth and therefore the largest stimulated tissue volume (green light is scattered less than blue light but strongly absorbed by blood). A suitable and truly red-sensitive opsin is now available: Chrimson (Klapoetke et al., 2014).

Typically, optogenetic constructs not only contain an opsin but also carry a fluorescent reporter such as mCherry or eYFP. Because channelrhodopsins integrate into the membrane of the cell, the linked fluorescent protein tag is also localized to the membrane. Because of the high membrane-to-volume ratio of neuropil compared with the cell body, the histological identification of opsin-positive cell bodies is extremely difficult when using such constructs. This drawback significantly impairs the accurate estimation of colocalization of channelrhodopsin with histochemical markers. Novel constructs have been developed which permit cleavage of opsin and marker so that the marker remains in the lumen of the cell, which improves the identification of opsin-positive cells (Gradinaru et al., 2010). However, for experiments where the terminals of transduced cells are to be stimulated, the use of a classical construct might be preferable, given easier identification. Another potential concern is the metabolic burden and negative selection pressure against cells expressing exogenous proteins as discussed earlier, and this may argue for reexamination of non-tagged optogenetic constructs to minimize metabolic load (Glick, 1995), especially for potential long-term or clinical uses.

To transduce VTA cells, AAV viral vectors are the most popular choice. Lentiviruses can be used for specific questions, but their toxicity, lower transduction efficiency, temperature sensitivity, and enhanced biosafety requirements make them a suboptimal choice for many *in vivo* experiments (Diester et al., 2011). AAVs can be purchased from the vector cores of various universities (e.g., University of North Carolina, University of Pennsylvania) or manufactured locally. Because high purity preparations are available from vector cores and the process is complicated and prone to technical pitfalls, we recommend the purchase of all standard vectors, if possible. For VTA stimulation, the AAV5 serotype in particular provides a good combination of spread, transduction efficiency, expression strength, and low overexpression. AAV8 shows higher expression levels

but may therefore also be more toxic. A concentration of 1×10^{12} viral particles per ml is recommended for experiments, but optimally, a dilution study is performed before the experiment to optimize the balance between expression strength and cell death for the particular biological application.

2.3 Choosing Fiber-Optic Implants

A number of different approaches for light delivery have been described in optogenetics. The earliest approach was the insertion of a bare optic fiber through a guide cannula (Zhang et al., 2010). Because this approach requires repeated insertion and removal of the fiber, it is associated with high risk of infection, cannula clogging, and fiber damage. A more recent approach is to use an implanted fiber inside a ferrule—a drilled cylinder with precise internal and external diameters—made from steel or ceramics. The ferrule holds and centers a short piece of fiber chronically inserted into the brain and allows accurate and precise mating of this fiber stub to a second ferrule and fiber external to the animal, which carries the stimulation light (Yizhar et al., 2011). Ferrules have the advantage that animals can be readily connected to and disconnected from the stimulation apparatus. An alternative, a mating sleeve, is a very simple way to achieve robust connection. Mating sleeves are hollow ceramic cylinders precisely matching the external diameter of the fibers. Mating sleeves, however, require a significant amount of force to connect fibers and are therefore prone to break, which can scratch and damage the delicate polished fiber surfaces. Given these concerns, our method of choice is to use auto-aligning magnetic connectors housing ferrules. These magnetic connectors are stable, do not lead to fiber-end scratching, automatically pull fiber ends tightly together, have zero insertion force, and do not commonly break.

Depending on necessary quantity and available funding, ferrule fiber implants and magnetic connectors can be either purchased (e.g., Thorlabs, Doric Lenses) or manufactured in-house. Manufacturing leads to prices around 10 USD per implant, whereas purchasing can be significantly more expensive.

To manufacture bare ferrule and magnetic implants, a suitable optical fiber is first glued into an empty ferrule (available from Thorlabs). Commonly, high OH silica step-index fibers with diameters of around 200 µm and a numerical aperture (NA) between 0.2 and 0.4 are used (e.g., Thorlabs FT200UMT, Thorlabs, Newton, NJ, USA). The diameter and NA must be larger than or equal to those of the fiber leading from the laser to the implant. The epoxy glue which holds the fiber inside the ferrule should have a high hardness for optimal polishing results (e.g., Thorlabs 353NDPK). It is also possible to use a light-curing cyanoacrylate glue (e.g., Loctite 4305, Henkel, Düsseldorf, Germany), which results in lower costs and more rapid fabrication, especially for lower numbers of manufactured implants. A detailed guide for the termination and polishing of optic fibers in ferrules is available from Thorlabs (FN96A). During the polishing process of the fiber, it is critical to regularly check the surfaces of the fiber and the ferrule. Pitting can result from overpolishing with coarse abrasives, and scratching can result from dust particles. These problems must be avoided in addition to the problem of underpolishing, where the fiber still protrudes from the ferrule. Such protrusion can lead to damage of both the implant as well as the connection cable, resulting in unreliable results which may not be immediately detectable. Following polishing, the fibers can be cut to the desired length (mouse: 6 mm, gerbil: 8 mm, rat: 10 mm) and potentially glued into the magnetic implant housing. Our implant housings are milled from metal or polyether ether ketone plastics (Fig. 17.1D). A computer-aided design (CAD) file for milling is available from the authors on request. Strong and very small neodymium magnets are now available for negligible cost (e.g., S-02-02-N, supermagnete.de, Gottmadingen, Germany).

2.4 Surgical Procedures

Injection of the VTA with an opsin construct and implantation of a fiber takes approximately one to one and a half hours per animal. As described in the following section, it is particularly important for optogenetic stimulation to achieve precise and accurate targeting of the injection and the fiber and to ensure firm fixation of the implant to the skull. We recommend the following procedure:

- Anesthetize the animal with sodium pentobarbital (rat and gerbil: 50 mg/kg, mouse: 55–60 mg/kg) following brief induction in 2%–3% isoflurane. Monitor for respiratory depression, as metabolic damage to the brain from hypoxia, hypercapnia, and hypotension can lead to occult behavioral issues in rodents. If anesthesia is too deep at any point, somatosensory stimulation may be applied to ensure a light but well-anesthetized state. Subcutaneous injections of saline are well suited for this purpose in rodents, compensate for insensitive and overt volume loss, and also support blood pressure homeostasis if the subject is properly urinating.
- Once pentobarbital anesthesia is fully induced, withdraw virus solution from an aliquot into a drawn

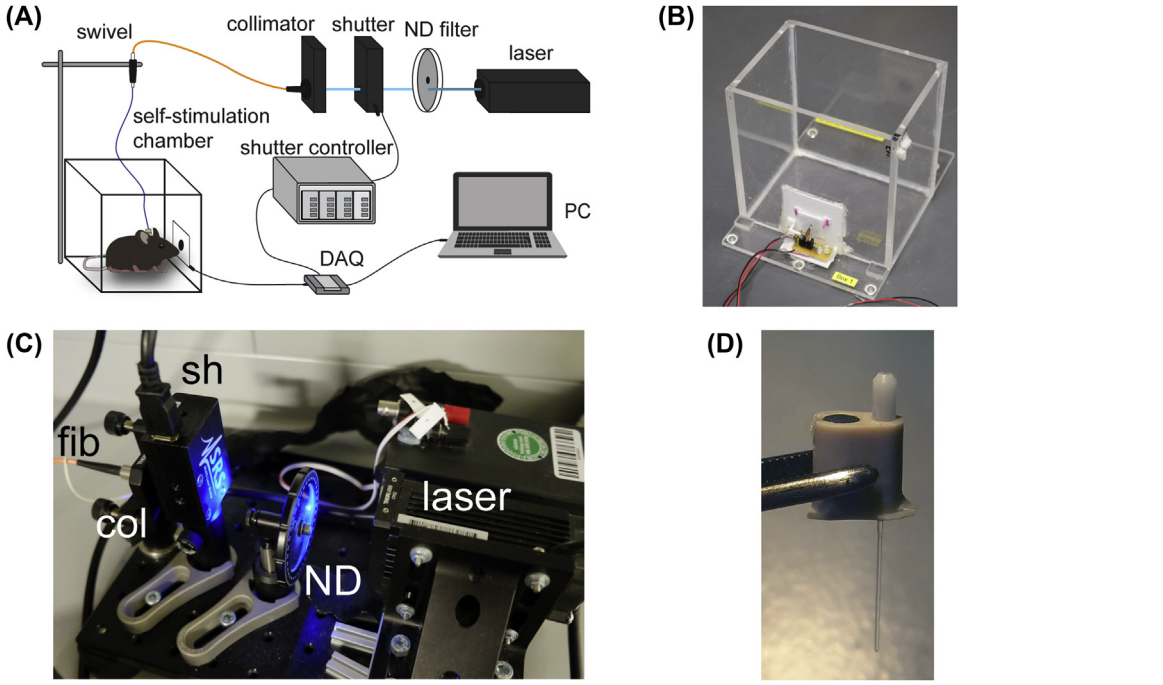

FIGURE 17.1 (A) Overview of our set-up for self-stimulation experiments. (B) Self-stimulation chamber with 3D-printed nose poke. (C) Detailed schema of optical beam path. The laser is attenuated by a variable neutral density filter (ND) and mechanically shuttered (sh). A collimator then focuses the free space beam into the optical fiber (fib), which connects to the animal. (D) Magnetic fiber implant for quick and effortless connection of the animal.

glass pipette using a volume-controlled microliter injector (e.g., WPI Nanoliter 2000, Drummond Nanoject). Withdraw approximately 20% more than the desired injection volume. Glass pipettes are much thinner than even the finest metal injection cannulas and should be used to minimize tissue damage. To achieve the necessary lengths for deep brain injections, use a pipette puller with a large heating zone (>5 mm) and adjust pulling parameters to obtain the desired shank profile.

- Shave the head of the animal and apply a bland eye ointment for protection, such as panthenol salve. Remaining hairs are a major cause of problems in wound healing, especially in rodents, so the incision area should be shaved particularly carefully, and loose hairs should be completely removed from the operating theater.
- Inject a longer acting local anesthetic subcutaneously in the area of incision (e.g., bupivacaine 0.25%). This allows maintenance of a light but stable anesthetic plane during the incision and subsequent cleaning, which are the points of maximal somatosensory stimulation in this procedure.
- Place the animal on a regulated heating pad and fix its head in a stereotactic frame. Improper fixture is the most common cause of unreliable targeting and of middle ear damage and other related undesirable behavioral outcomes.
- Incise with one cut along the midline using a sharp scalpel. Blades should not be reused. Dull blades or scissor usage causes blunt trauma, leading to delayed wound healing. Expose the dorsal surface of the skull from the cerebellum posteriorly to beyond bregma anteriorly.
- Clean the exposed surface thoroughly with cotton swabs and hydrogen peroxide (3%). If bleeding or oozing from cortical arteries is present, use a small amount of bone wax to close them because such bleeding will only increase as the animal awakes from surgery and the blood pressure rises. However, excess wax may cause problems with implant adhesion if not cleaned carefully. In rats, cauterization of bone vessels may occasionally be necessary for atypically large blood vessels and animals with hypertension. If cauterizing, use extreme caution to avoid heat damage to the brain.
- Once the surface is cleaned, dry briefly using a gentle stream of compressed air. The surface of the skull must be completely white and consist of mineralized bone, free of periosteum and blood. Thoroughly scratch the surface with a sharp scalpel blade to form a fine hatched pattern. When done correctly, this roughening provides critical adhesive stability of the head cap.
- Make sure no liquids seep into or out of the scratched patterns. If this happens, reclean with hydrogen

peroxide and dry. Apply a drop of Vetbond (3M, Maplewood, MN, USA) or similar cyanoacrylate adhesive, spread it over the whole area, and let it dry to further prevent moisture from weakening the skull–implant interface. If this procedure is followed, bone screws may be unnecessary for more simple implants.

- Mark lambda and bregma using a fine ink marker. The identification of these points is often done incorrectly, leading to excessive variability in stereotactic placement. It is important to use the intersection of imaginary best-fit lines along the bone sutures (Fig. 17.2) instead of the actual anatomical *lambda* and *bregma* points, which have a higher anatomical variability in relation to the underlying brain structures.
- Adjust the bite bar so that *lambda* and *bregma* are at the same height (less than 100 μm deviation)
- Mark the position of the drill hole (for coordinates see Fig. 17.2A) and drill carefully through the skull using a stable dental drill (burr with approximately 800 μm). We prefer carbide burrs due to their sustained sharpness. Drill carefully and avoid damage to the cortical surface but ensure that lateral clearance of the walls of the drill hole is sufficient to accommodate the full thickness of the injection capillary and the optic fiber, without contact and bending.
- Using a slightly bent syringe needle tip, nick the dura mater.
- Place injector in a stereotactic holder and record *lambda* and *bregma* positions. For rats, brain coordinates should be scaled based on the distance between these two points.
- Place tip of injector over the drilled hole and confirm durotomy using the slightly bent syringe needle tip.
- Inject desired volume (mice: 500 nL, rats: 650 nL gerbils: 650 nL) at the depth of the VTA (Fig. 17.2A, depth is measured from dura). Use a flow rate of 50–100 nL/min; exceeding this rate can lead to tissue damage.
- Leave cannula in place for 5 min to let virus solution diffuse into the surrounding tissue and then withdraw cannula.
- Exchange injector holder with a fiber holder. Reconfirm stereotactic coordinates relative to *bregma* or *lambda*. In our experience, simply using the hole as a guide for fiber placement saves little time, but may reduce experimental yield significantly. This reconfirmation also serves as a sanity check for this critical step.
- Slowly insert the fiber into the brain. The final position should be 300 μm above the most dorsal injection site or directly at the dorsal boundary of the VTA. Protect the margin around the fiber with a small drop of cyanoacrylate and cure for 5 min.
- Secure the fiber implant to the skull using dental cement which has been rendered opaque with fine charcoal powder (e.g., 05105, Sigma–Aldrich, St. Louis, MO, USA), which blocks stray light.
- Remove fiber from holder after the cement has set.
- Wound margins can be fixed around the head cap using cyanoacrylate adhesive (3M Vetbond). Although this step violates basic surgical principles of wound closure, it is necessary given the unavoidable presence of a foreign material (the head cap), as well as the special circumstance in rodent surgery that the wound cannot be completely protected from grooming (wound dressings or Elizabethan collars are usually not quite practical in rodents, given their size). As a rule, wound margins should not come into direct contact with dental cement or any other caustic materials which are overtly tissue toxic because this will impede proper wound healing and raise the risk of pain, infection, or generalized inflammatory states from development. Remove the animal from the stereotactic frame and place in a heated home cage. Litter should be removed from the cage or isolated with a paper towel to prevent aspiration during early stages of arousal. Saline may be injected subcutaneously to support

(A)

	AP	ML	DV
Mouse	-3.5	-0.4	-3.7
LE-Rat	-5.8	-0.7	-6.8
Gerbil	-4.0	-0.5	-6.2

(B)

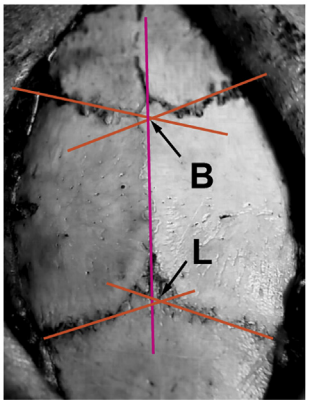

FIGURE 17.2 (A): Table with stereotactic coordinates for fiber positions in different species. We use TH-Cre transgenic Long–Evans rats and DAT- and TH-Cre transgenic C57/Bl6J mice. Injections are performed approximately 300–500 μm deeper than the given fiber positions. Depths are relative to the dural surface. (B) *Lambda* and *bregma* are determined with best-fit lines derived from bone sutures and not from the true anatomical *lambda* and *bregma* points, which are more variable between animals. AP: anterior-posterior; ML: medial-lateral; DV: dorsoventral.

recovery if the animal has urinated significantly or if the air is dry and insensitive loss is a concern.
- Monitor the animal for the following hours, providing analgesia (e.g., Meloxicam 0.2 mg/kg i.p., Buprenorphine 0.05 μg/kg i.p.).
- Before new experimenters or new equipment are introduced to the workflow, we recommend performing a mock surgery with a concentrated solution of DiI (Sigma−Aldrich, St. Louis, MO, USA) in ethanol instead of virus (50 μL per site). Instead of implanting a cannula, the animal is perfused immediately after dye injection and the brain sliced on a vibratome. The brightly visible red marks help to confirm stereotactic coordinates and to calibrate technique if necessary.
- Following stereotactic surgery, the animals should be left to recover and express opsin for at least 2 weeks. We prefer 3 weeks for the constructs mentioned here, and we have not observed any significant decline in self-stimulation behavior for at least 8 weeks.

In our experience, the use of a digital or computerized stereotactic frame can help to improve targeting accuracy and reduce surgical time (Neurostar Robot or DigiW, Neurostar, Tübingen, Germany); such accuracy is particularly beneficial for optogenetic stimulation compared with, for example, electrical stimulation or pharmacological injections because stimulation light is highly localized in the tissue. It should be noted, however, that such devices are expensive and often require close monitoring and maintenance by an experienced experimenter. Short of expensive robotic systems, digital read-out calipers can be retrofitted to existing stereotactic frames by a competent workshop and provide many of the same benefits.

Unilateral surgery and stimulation is sufficient to elicit vigorous self-stimulation. We therefore prefer this over bilateral stimulation, as it is often unclear with bilateral stimulation if both stimulated sides are indeed functional in self-stimulation and dopamine release.

2.5 Self-Stimulation Set-up

The set-up for self-stimulation training consists of the following main parts: a light source with optical shutter, optical cable with commutator, self-stimulation chamber with nose poke, and data acquisition system (Fig. 17.1A).

2.5.1 Light Source

For self-stimulation, laser light sources are advantageous. They easily provide enough power reserve to output 20 mW from a 200 μm NA 0.4 fiber. Hence, the laser should have at least 50 mW of rated power to accommodate optical losses and laser aging. If a diode-pumped solid-state (DPSS) laser is selected, which is the most affordable option, a laser with 5% or better stability should be used because the rating characterizes root mean square fluctuations which momentarily exhibit phases of much greater changes. This behavior is normal for DPSS lasers, which undergo frequent laser mode changes which can result in large, unpredictable power fluctuations. In addition, DPSS lasers need a warm-up time and therefore, should not be pulsed. Instead, the laser should be run in continuous mode and optically shuttered.

Diode lasers are more stable and can be pulsed directly but often show unpredictable mode hopping problems from back reflections in the optical pathway. In such a case, the output power measured during calibration at the fiber tip can be completely different from what the laser delivers when it is attached to the animal. It is therefore advantageous, in the case of diode lasers, to use a system with active optical feedback or a system with active mode hopping suppression (e.g., iBeam, TOPTICA, Gräfelfing, Germany). The power of the laser can either be adjusted through the driver or for highest stability, with a variable neutral density filter in the beam path. Mechanical shuttering of the light beam can be achieved with high-speed shutters (SR470, Stanford Research Systems, Sunnyvale, CA, USA). Shutters for microscopes or light guide sources should not be used due to their slow speed and loud actuation noise.

The optical cable which connects the laser system and the animal should be commutated to allow the animal to turn freely. VTA stimulation in particular can cause increased locomotion in the animal, in a manner reminiscent of psychomotor agitation. A commutator can prevent the fiber from twisting and thereby preventing the animal from pressing the nose poke. For mice, it is advisable to use a commutator with low resistance to turning (e.g., FRJ, Doric Lenses Inc., Quebec, Canada).

Optical commutators may not be necessary for LED-based stimulation systems, which can be electrically commutated (e.g., PlexBright, Plexon Inc., Dallas, TX, USA). LED systems also allow a linear regulation of intensity and have none of the problems associated with the coherent radiation of a laser. However, currently available LEDs cannot deliver the necessary brightness to couple 10 mW of illumination into a 200 μm N.A. 0.4 fiber. Instead, available commercial LED systems use thicker fibers or higher NAs. This broadens the light cone exiting the fiber and therefore only marginally increases irradiance at the target cells. It may therefore stimulate a larger tissue volume ineffectively instead of stimulating a smaller volume effectively. At the time of writing, we therefore rather recommend laser-based systems for applications similar

to those described in this chapter. Should an LED system be the only available option, we recommend implanting the thicker fiber directly into the VTA instead of slightly above it to maximize the chances of successful stimulation.

2.5.2 *Self-Stimulation Chamber*

Our self-stimulation chambers are made of plastic and have the following dimensions for mice: 150 × 110 × 150 mm (width, depth, height, nose poke height 25 mm) and rats and gerbils: 250 × 220 × 350 mm, nose poke height 60 mm. A lid with a central hole of half the total aperture size permits access for the fiber optic cable, yet prevents animals from jumping out. Make sure that all box edges are well rounded, as sharp edges may damage the fibers. Our boxes also feature a detachable magnetic front panel so that it can be thoroughly cleaned between sessions.

Animals can elicit stimulation by pressing a nose poke lever in the front. Different types of levers, wheels, and nose pokes are possible. However, in our experience, a low actuation force mechanical nose poke (i.e., a lightweight flap that the animal pushes inward with its nose) is the most naturalistic and easiest to learn. In comparison to a purely optical nose poke, where the animal pokes into an open hole and breaks a light beam, a mechanical nose poke provides clear feedback to the animal about the action of the trigger. The registration of presses is achieved with an optical switch triggered by a small protruding part at the rear of the nose poke flap. An optical switching mechanism requires no actuation force, in contrast with a mechanical switch or lever. We believe that this leads to more accurate reflection of the animals' intent to initiate a press. The apparatus was designed in a CAD program and 3D printed (files are available from the authors on request). The resulting nose pokes are therefore identical and interchangeable between boxes. Inter-chamber similarity is especially important in studies requiring parallel training of multiple animals. The circuit diagram of the optical switch and CAD files for printing are available from the authors on request.

A computer coupled to a low-cost USB DAQ (data acquisition) system (USB-6008, National Instruments, Austin, TX, USA) can be used to interface the laser and the nose poke. The DAQ system monitors the optical switch and on opening, the computer triggers playback of the required stimulation waveform from the DAQ device, which is sent to the laser or laser shutter (Fig. 17.1A). Given the biological timescale of the nose poke action itself, which is on the order of hundreds of milliseconds, it is completely unnecessary to use an expensive real-time system for this stimulation, although the DAQ system output for pulse trains should be hardware buffered and accurate. One can easily achieve sub-ms timing in modern desktop computers by (1) using a system with six or more cores, (2) setting thread priorities correctly, (3) disabling background processes (especially virus scanning, windows search, and network-related interruptions), and (4) observing idiomatic programming practices. However, modern logging mechanisms should also be put in place to notify the experimenter if a stimulation may have been significantly delayed. If the system is programmed properly, this should never happen, but we have experienced problems especially with Windows updates, which are necessary for system security, but which can lead to intense, high priority CPU threads. We therefore recommend that network connections and monitoring software such as Windows Defender should be disabled on DAQ systems for the duration of active experiments.

Time-outs are an important factor in programming such stimulation but are rarely specified in the literature. We generally use a time-out which is as long as the pulse train in question, and nose poke presses which occur during the time of active stimulation are not reinforced. When comparing results of very long pulse trains and very short pulse trains, this may affect the interpretation of behavioral results, especially when the animal is stimulating at very high rates. This is also discussed in the next section.

2.6 Self-Stimulation Training

Self-stimulation training starts with a careful inspection and calibration of the optical system. The laser should have been given time to warm up (10 min) to stabilize output power.

- Wear suitable eye protection while lasers are active.
- Check all optical and electrical cables. They should be connected and without damage. Problems with cables and cable connections are one of the most common sources of occult errors during experiments.
- Open the shutter or switch diode laser to CW mode and measure output power at the end of the optical cable with optical power meter (PM121D, Thorlabs Inc., Newton, NJ, USA). Adjust to desired value (e.g., 10 mW) using a variable neutral density filter. Observe the shape of the light disk on a flat surface and make sure it is round and homogeneous, i.e., that the light path is well centered. This step is critical. It is insufficient to simply measure once at the beginning of a study or just accept the manufacturer ratings.
- Close shutter or switch diode laser into triggered mode.
- Take the animal from its home cage, let it hold onto the upper edge of the box, make sure that the fiber end is clean, and carefully connect the fiber optic cable.

- Place the animal into the self-stimulation chamber.
- Start self-stimulation script (available from the authors on request) and set run time to 20 min. Stimulation parameters are discussed in the next section.
- Ideally, the animal should be monitored remotely during the experiment using a camera.
- After 20 min of self-stimulation, save recorded press rate and time stamps.
- Remove the animal from the chamber and place in the home cage.
- Thoroughly clean the chamber using rubbing alcohol or another suitable cleaning solution. Eliminate or potentially mask the scent of previous animals before conducting next experiment.
- Repeat procedure for 10 days and monitor learning curves.

Depending on the experimental question, one or two habituation sessions can be done before training in the same box with access to the nose poke blocked, but is not necessary to obtain the types of behavioral curves described in this chapter. Animals should show signs of significant self-stimulation by day three at the latest, given reasonable parameters and good preparation. Strong self-stimulation behavior does not usually occur immediately from the beginning of training, as is often the case with electrical intracranial stimulation paradigms. In the first training sessions, the animals will spend more time exploring the self-stimulation chamber and not press as vigorously. However, during about 10 days of daily training, press rates will increase until they settle for a value which is characteristic for a particular animal. When plotted in a learning curve, individual animals as well as a population of animals will often show a continuous increase of press rates over days.

A pressing rate (as defined as the number of presses in total, including multiple presses during stimulation, which do not lead to new stimulus delivery) of about once per minute is the background rate at which an exploring animal presses the lever by chance. A rate above 10 presses/min indicates successful stimulation, but some animals can reach up to 100 presses/min, depending on pulse train parameters.

Typically, pressing is organized into bouts. For more vigorously stimulating animals, these can turn into virtually constant pressing. Occasionally, an animal may "lose interest" in self-stimulation and sit in a corner for extended periods of time, leading to lower rates than expected from a true reflection of the learned operant. This variability can be minimized with standard practices such as conducting behavior at the same time each day by the same experimenter under the same environmental conditions and by avoiding fighting, cage changes, and other stressors in animal housing. Careful checking of the apparatus, as described earlier, is also crucial for experimental stability.

Many different methods have been described in the literature for analysis of self-stimulation behavior evoked by electrical stimulation and are mostly applicable to optogenetic stimulation as well (Negus and Miller, 2014). One method that captures the nature of optogenetic self-stimulation with a free-pressing paradigm such as ours is to fit the learning curve with a growth model. The Gompertz growth model, in particular, has been optimal for this purpose (Coulombe and Miliaressis, 1987; Ranaldi et al., 1994)

$$R = ae^{-e^{(b-cX)}}$$

In this model, R is the response strength in lever presses and X is the independent variable, for example, session number, stimulation frequency, number of pulses in the train, optical power of stimulation light, etc. By fitting the model to the data, various measures can be obtained with more reliability compared with direct inference from individual raw values (e.g., self-stimulation threshold, inflection point, 75% of maximum). This approach is particularly valuable when the quantification of the intensity of self-stimulation behavior is important, for example, for power titrations to apply comparable powers to different animals.

2.7 Choice of Stimulation Parameters

Virtually all types of optogenetic VTA stimulation will result in self-stimulation behavior. In general, tonic (Kolodziej et al., 2014) and phasic excitation (Helbing et al., 2016) can be used. Tonic stimulation induces more desynchronized firing patterns (Guru et al., 2015), whereas phasic excitation mimics the burst discharges that are characteristic for VTA neurons responding to unexpected reward (Trulson and Trulson, 1987). Examples for neuronal responses to tonic and phasic stimulation are shown in Fig. 17.4. Of note, tonic stimulation induces the strongest response at stimulation onset. In the VTA, subsequent activity is partially inhibited. Phasic stimulation on the other hand induces a burst of neuronal discharges with each laser pulse. One study explored the parameter space of optogenetic VTA stimulation (Ilango et al., 2014a,b). In general, frequencies around 25 Hz are ideal for effective stimulation, evoke the strongest self-stimulation behavior, and are also commonly used in optogenetic VTA stimulation studies (Ferenczi et al., 2016; Helbing et al., 2016; Lohani et al., 2017). Frequencies far above 25 Hz should be used with caution, as the cells in the VTA cannot follow faster stimulation well (Ilango et al., 2014a,b). If such frequencies are needed, care should be taken to confirm

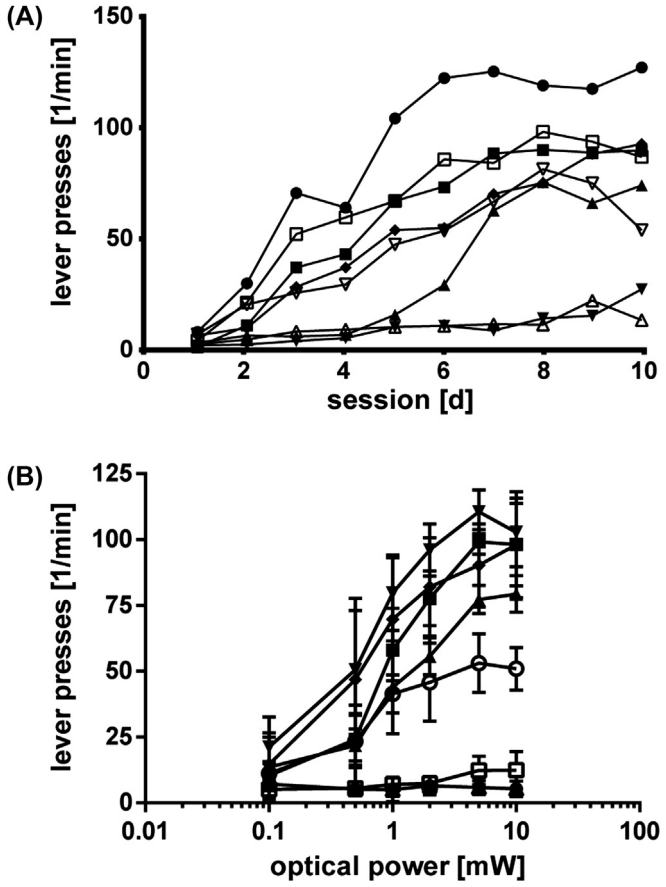

FIGURE 17.3 (A): Self-stimulation learning curves for several TH-Cre rats. Lever pressing is acquired progressively over approximately 10 days. Each animal approaches a characteristic stimulation rate at which it will remain stable over time for a given set of stimulation parameters. A predefined threshold can be used to exclude nonresponders (e.g., 10–20/min). (B) After learning, self-stimulation rate increases with increasing laser power in a logarithmic manner. Very weak laser powers are already sufficient to induce significant lever pressing. Maximal rates are achieved at approximately 10 mW optical power.

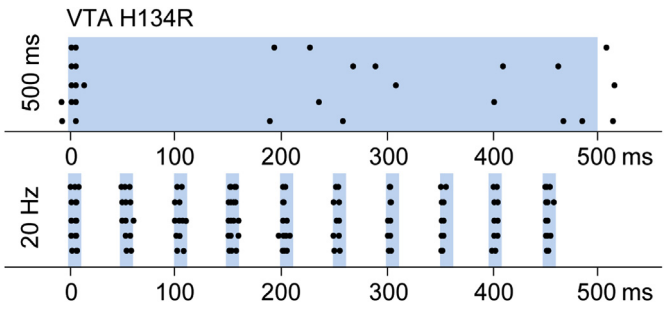

FIGURE 17.4 Multiunit responses recorded with an optrode from the ventral tegmental area (VTA) of a DAT-Cre mouse. Tonic stimulation (top panel) leads to phasic spiking activity at light onset, approximately 200 ms of suppressed spiking, and irregular spiking afterward. Phasic stimulation with 10 ms light pulses at 20 Hz results in time-locked phasic spiking to each pulse. Despite the total amount of light being significantly larger during tonic stimulation, phasic stimulation results in more spikes per time interval.

the effects of stimulation through simultaneous extracellular electrophysiology.

The number of pulses in each pulse train should be kept at approximately 5 to 10 pulses, as a rule of thumb. Fewer pulses lead to weaker self-stimulation behavior (Ilango et al., 2014a,b), whereas more pulses lead to stronger self-stimulation but limit the hypothetically possible maximal stimulation rate.

Optical power has a very strong influence on self-stimulation behavior (Fig. 17.3B) and can be adjusted continuously across a wide range. Up to a certain power, the press rates increase, and they saturate at a characteristic value for each animal. Ideally, one would apply as much optical power as available. However, laser light at the intensities used leads to significant brain heating (Arias-Gil et al., 2016). This issue is especially problematic because the animal might be exposed to almost constant illumination for 20 min if it shows strong self-stimulation behavior. Should brain heating cross a threshold of around 6 K for too long, brain tissue might be permanently damaged (Thomsen, 1991). Values around 2 mW, far below this limit, might already increase cell excitability in a nonspecific manner due to thermal effects. To estimate the heating caused by a particular pulse paradigm, we have published an online calculator at our laboratory website (Arias-Gil et al., 2016). Thermal damage from excessive light is depicted in Fig. 17.5B. Practical values for power are in the range of 10 mW for 10 ms pulses and 20 mW for 5 ms pulses delivered at 25 Hz. Utmost care has to be taken to avoid accidental shutter opening while the animal is attached to the light source. Exposure to continuous wave laser illumination can destroy the transduced tissue within seconds.

In terms of behavior, self-stimulation is associated with exponential phases at the beginning and end of stimulation. During the first minutes of a session, animals will increase their pressing rates. If the animal is left in the chamber but not provided with stimulation, pressing will exponentially seize within a few minutes. A certain minimum duration of stimulation is therefore necessary to obtain a stable read-out of self-stimulation behavior. A practical value would be 10 min of stimulation. For the initial training of self-stimulation, we use a duration of 20 min per session and day.

2.8 Histological Confirmation of Opsin Expression and Fiber Placement

On completion of the experiment, animals should be perfused and the brain extracted for histological analysis. For perfusion, we prefer a preprepared phosphate-buffered formaldehyde solution (e.g., 4%, AppliChem, Darmstadt, Germany) to minimize workplace

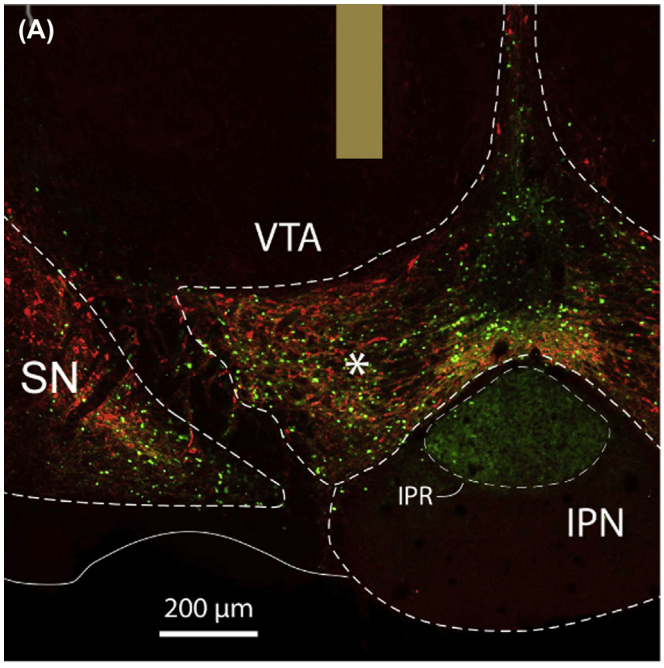

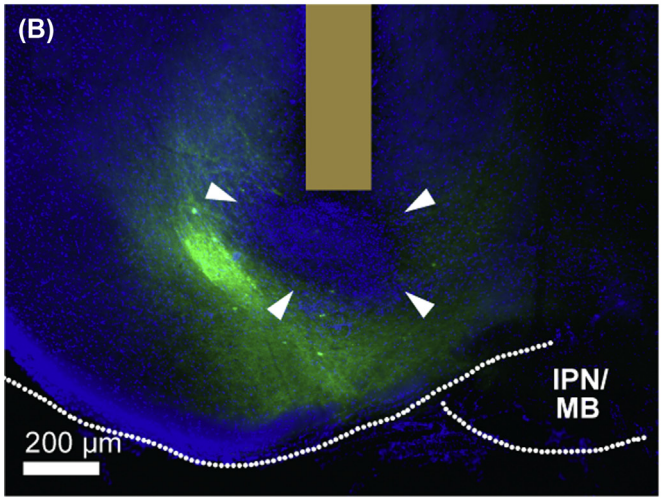

FIGURE 17.5 (A): Histology of a fiber implantation site in a TH-Cre mouse. Opsin expression (green) is present in the ventral tegmental area (VTA) and substantia nigra (SN), where it partially overlaps with anti-TH staining (red). Expression is also seen in the nondopaminergic interpeduncular nucleus (IPN). In the DAT-Cre mice and TH-Cre rats used in this chapter, such ectopic expression is not present. The fiber is implanted about 300 µm dorsal to the VTA. (B) Damage from excessive light. Opsin expression (visible as green fluorescence) is eliminated directly below the fiber, and instead, an increase in nuclear density is seen (DAPI stain, blue; presumably gliotic).

safety risks. After perfusion, the brain should be left in the same solution for 12 h and sliced on a vibratome. Alternatively, a cryoslicing protocol can be used that contains a cryoprotectant (sucrose). Flash freezing is not recommended, as the fluorescent marker of the opsin may diffuse during thawing/mounting without proper fixation and cryoprotection. To confirm the dopamine specificity of the stimulation, we stain selected slices with anti-TH antibody in a standard manner (e.g., primary 1:1000 polyclonal rabbit anti-TH, Abcam ab112, fluorescent secondary anti-rabbit antibody Abcam ab6939, Fig. 17.5A). As mentioned earlier, opsins that are still linked to the fluorescent tag accumulate in the membrane, and costaining of tag and anti-TH antibody is difficult to assess. Constructs containing a p2a-cleavage sequence, causing tag and opsin to separate, might be preferred for this purpose.

3. PITFALLS AND TROUBLESHOOTING

There are several critical points within the experiment. The following list should guide the troubleshooting process:

Surgical Problems:

- Surgical wound is inflamed or infected: make sure the surgery is done under clean conditions. Sterilize instruments and hands and clean skull surface very carefully. Incisions should be made with a sharp scalpel, and never with scissors, as is often done by inexperienced experimental surgeons. The blunt force applied to tissue edges will cause crush trauma and impede proper healing. Pay attention to sealing of wound margins, and properly suture apposed cuts or use tissue glue. Avoid caustic materials such as dental acrylic on open wound surfaces. Note that given the viral infection cycle, systemic inflammatory states caused by poor wound management and postsurgical recovery could very well affect correct viral transduction, as is clinically well known in the context of viral encephalitis.
- Implants fall off: Invasion of serum, blood, or tissue fluid under the implant, especially during the initial curing process, is the most common cause of poor implant attachment. In particular, the skull surface may not be cleaned well enough or the scull roughening as described previously may be insufficient. Skull screws may be indicated if the problem persists, especially with larger, more complicated implants.

Problems During Self-Stimulation Training:

- Animals do not show self-stimulation behavior:
  Either the light does not sufficiently activate transduced cells, or there are not enough effectively transduced cells. Confirm expression of ChR2 and fiber position in histological slices. Fluorescence should be brightly visible. Excessive numbers of bright spots in the tissue can indicate damaged cells

or cell death due to overexpression. If no expression is present, it is likely that the viral solution did not reach the target tissue. Make sure that the injection cannula is not clogged. Consider a different virus or conduct a dilution study with different dilutions of the virus. If a recombinase approach is used, confirm stereotactic placement again with the dye DiI, as the virus will not express if the VTA is not correctly targeted. Proper perfusion of the brain before extraction is important to accurately determine fiber position in histological slides.

If expression is present, but animals do not show self-stimulation behavior, incorrect placement of the fiber is a likely culprit. Given the short penetration of light wavelengths commonly used, the fiber must be placed very close to the VTA or inside the VTA for the stimulation to be effective. Some extent of stereotactic inaccuracy at this level may be unavoidable, and a number of animals will often not show self-stimulation due to this. This should be taken into account during the planning of a study. An unlikely, but possible, reason for failure to acquire self-stimulation can be the chamber size of the self-stimulation apparatus. If the chamber is excessively large or if the animal is in distress, it may not operate the nose poke by chance often enough to learn its appetitive characteristics within a reasonable time frame. Therefore, confirm that a low baseline press rate of around 0.5 to 1 press per minute is present.

A further technical reason for lack of self-stimulation may be a damaged optical path. Ensure that the implant is not damaged and sufficient light enters it. High-NA patch cables in particular are quite finicky and break easily, resulting in a markedly reduced power output.

- Animals show only low self-stimulation behavior:

  Confirm viral expression. If expression is confined to a small area or if the expression is weak, sparse, or shows signs of overexpression, adjust volume of injection and consider different dilution or serotypes (AAV5 and AAV8 work well). Confirm fiber placement. A large distance between VTA and fiber end will lead to insufficient stimulation brightness at the target. Confirm with a photodiode (BPW34, Osram, Munich, Germany) that light pulses have the desired shape. Slow shutters can cause problems due to insufficient aperture opening as well as directly TTL-pulsed DPSS lasers. Such problems cannot be detected during standard calibration with continuous laser intensity measurement. In addition, confirm that the animals can press the nose poke lever effortlessly and that the DAQ system correctly reports each press.
- Press rates drop at some point in the experiment and do not recover:

  This pattern is typical for heat or blue light damage to the stimulated site or movement of the implant. Make sure optical power is appropriate and delivered accurately. Lasers show aging and mode hops, and the optical cable can be easily damaged. Check that fiber surfaces are clean and not scratched or broken. Confirm the stability of the head cap and implant. Conduct a search for tissue damage below the fiber during histology (Fig. 17.5B).
- Press rates fluctuate between days:

  Optical power of the light source is unstable, connection of light source and animal is unstable, or surfaces are dirty. Measure optical powers and confirm proper connections. In addition, there may be a general problem with animal state (e.g., distraction) or with the set-up. Make sure that the animal is not disturbed during the stimulation, does not show overt signs of illness, and confirm that the chamber is cleaned properly. If multiple chambers are used, always test each animal in the same chamber. Confirm correct operation of the nose poke lever. Although the abovementioned issues should eliminate the majority of significantly fluctuating behavior, some fluctuations may be unavoidable due to practically uncontrollable changes in the hormonal or motivational state of the animal.
- Animals show rotational bias:

  Excessive rotations of the animal in one direction are typical for activation or for damage (viral, heat, or surgical damage) to the basal ganglia system, in particular the SNc. Confirm that the stimulation location is not too lateral. SN stimulation can also induce self-stimulation behavior; therefore the fiber and injection locations should be carefully confirmed using histology.

CONCLUSIONS

Optogenetic intracranial self-stimulation is a helpful tool to study the plasticity-inducing effects of dopamine release in the brain. In contrast to electrical stimulation, optogenetic stimulation allows to specifically target selected cell populations. However, the method has a number of properties which often cause experimental difficulties. In this chapter we have addressed these issues allowing other scientists to adapt the method for their specific research questions.

References

Adamantidis, A.R., Tsai, H.-C., Boutrel, B., Zhang, F., Stuber, G.D., Budygin, E.A., et al., 2011. Optogenetic interrogation of dopaminergic modulation of the multiple phases of reward-seeking behavior. J. Neurosci. 31 (30), 10829–10835. https://doi.org/10.1523/JNEUROSCI.2246-11.2011.

Akram, H., Miller, S., Lagrata, S., Hyam, J., Jahanshahi, M., Hariz, M., et al., 2016. Ventral tegmental area deep brain stimulation for refractory chronic cluster headache. Neurology 86 (18), 1676–1682. https://doi.org/10.1212/WNL.0000000000002632.

Al-Juboori, S.I., Dondzillo, A., Stubblefield, E.A., Felsen, G., Lei, T.C., Klug, A., 2013. Light scattering properties vary across different regions of the adult mouse brain. PLoS One 8 (7), e67626. https://doi.org/10.1371/journal.pone.0067626.

Arias-Gil, G., Ohl, F.W., Takagaki, K., Lippert, M.T., 2016. Measurement, modeling, and prediction of temperature rise due to optogenetic brain stimulation. Neurophotonics 3 (4), 45007. https://doi.org/10.1117/1.NPh.3.4.045007.

Aschauer, D.F., Kreuz, S., Rumpel, S., 2013. Analysis of transduction efficiency, tropism and axonal transport of AAV serotypes 1, 2, 5, 6, 8 and 9 in the mouse brain. PLoS One 8 (9), e76310. https://doi.org/10.1371/journal.pone.0076310.

Bäckman, C.M., Malik, N., Zhang, Y., Shan, L., Grinberg, A., Hoffer, B.J., et al., 2006. Characterization of a mouse strain expressing Cre recombinase from the 3′ untranslated region of the dopamine transporter locus. Genesis 44 (8), 383–390. https://doi.org/10.1002/dvg.20228.

Bao, S., Chan, V.T., Merzenich, M.M., 2001. Cortical remodelling induced by activity of ventral tegmental dopamine neurons. Nature 412 (6842), 79–83. https://doi.org/10.1038/35083586.

Boyd, E.S., Gardner, L.C., 1967. Effect of some brain lesions on intracranial self-stimulation in the rat. Am. J. Physiol. 213 (4), 1044–1052.

Boyden, E.S., Zhang, F., Bamberg, E., Nagel, G., Deisseroth, K., 2005. Millisecond-timescale, genetically targeted optical control of neural activity. Nat. Neurosci. 8 (9), 1263–1268. https://doi.org/10.1038/nn1525.

Budinger, E., Laszcz, A., Lison, H., Scheich, H., Ohl, F.W., 2008. Non-sensory cortical and subcortical connections of the primary auditory cortex in Mongolian gerbils: bottom-up and top-down processing of neuronal information via field AI. Brain Res. 1220, 2–32. https://doi.org/10.1016/j.brainres.2007.07.084.

Cardozo Pinto, D.F., Lammel, S., 2017. Viral vector strategies for investigating midbrain dopamine circuits underlying motivated behaviors. Pharmacol. Biochem. Behav. https://doi.org/10.1016/j.pbb.2017.02.006. S0091-3057(16)30318-5.

Cherepkova, E.V., Aftanas, L.I., Maksimov, N., Menshanov, P.N., 2016. Frequency of 3′ VNTR polymorphism in the dopamine transporter gene SLC6A3 in humans predisposed to antisocial behavior. Bull. Exp. Biol. Med. 162 (1), 82–85. https://doi.org/10.1007/s10517-016-3551-7.

Cooper, S., Robison, A.J., Mazei-Robison, M.S., 2017. Reward circuitry in addiction. Neurotherapeutics 14 (3), 687–697. https://doi.org/10.1007/s13311-017-0525-z.

Coulombe, D., Miliaressis, E., 1987. Fitting intracranial self-stimulation data with growth models. Behav. Neurosci. 101 (2), 209–214.

Decot, H.K., Namboodiri, V.M.K., Gao, W., McHenry, J.A., Jennings, J.H., Lee, S.-H., et al., 2017. Coordination of Brain-wide activity dynamics by dopaminergic neurons. Neuropsychopharmacology 42 (3), 615–627. https://doi.org/10.1038/npp.2016.151.

Deisseroth, K., 2015. Optogenetics: 10 years of microbial opsins in neuroscience. Nat. Neurosci. 18 (9), 1213–1225. https://doi.org/10.1038/nn.4091.

Delgado, J.M.R., Roberts, W.W., Miller, N.E., 1954. Learning motivated by electrical stimulation of the brain. Am. J. Physiol. 179 (3), 587–593.

Diester, I., Kaufman, M.T., Mogri, M., Pashaie, R., Goo, W., Yizhar, O., et al., 2011. An optogenetic toolbox designed for primates. Nat. Neurosci. 14 (3), 387–397. https://doi.org/10.1038/nn.2749.

Ellwood, I.T., Patel, T., Wadia, V., Lee, A.T., Liptak, A.T., Bender, K.J., Sohal, V.S., 2017. Tonic or phasic stimulation of dopaminergic projections to prefrontal cortex causes mice to maintain or deviate from previously learned behavioral strategies. J. Neurosci. https://doi.org/10.1523/JNEUROSCI.1221-17.2017.

Fenno, L.E., Mattis, J., Ramakrishnan, C., Hyun, M., Lee, S.Y., He, M., et al., 2014. Targeting cells with single vectors using multiple-feature Boolean logic. Nat. Methods 11 (7), 763–772. https://doi.org/10.1038/nmeth.2996.

Ferenczi, E.A., Zalocusky, K.A., Liston, C., Grosenick, L., Warden, M.R., Amatya, D., et al., 2016. Prefrontal cortical regulation of brainwide circuit dynamics and reward-related behavior. Science. https://doi.org/10.1126/science.aac9698.

Glick, B.R., 1995. Metabolic load and heterologous gene expression. Biotechnol. Adv. 13 (2), 247–261.

Gradinaru, V., Zhang, F., Ramakrishnan, C., Mattis, J., Prakash, R., Diester, I., et al., 2010. Molecular and cellular approaches for diversifying and extending optogenetics. Cell 141 (1), 154–165. https://doi.org/10.1016/j.cell.2010.02.037.

Guru, A., Post, R.J., Ho, Y.-Y., Warden, M.R., 2015. Making sense of optogenetics. Int. J. Neuropsychopharmacol. pyv079. https://doi.org/10.1093/ijnp/pyv079.

Harvey, J.A., Heller, A., Moore, R.Y., 1963. The effect of unilateral and bilateral medial forebrain bundle lesions on brain serotonin. J. Pharmacol. Exp. Ther. 140, 103–110.

Helbing, C., Brocka, M., Scherf, T., Lippert, M.T., Angenstein, F., 2016. The role of the mesolimbic dopamine system in the formation of blood-oxygen-level dependent responses in the medial prefrontal/anterior cingulate cortex during high-frequency stimulation of the rat perforant pathway. J. Cereb. Blood Flow Metab. 36 (12), 2177–2193. https://doi.org/10.1177/0271678X15615535.

Hjelmstad, G.O., Xia, Y., Margolis, E.B., Fields, H.L., 2013. Opioid modulation of ventral pallidal afferents to ventral tegmental area neurons. J. Neurosci. 33 (15), 6454–6459. https://doi.org/10.1523/JNEUROSCI.0178-13.2013.

Ilango, A., Kesner, A.J., Broker, C.J., Wang, D.V., Ikemoto, S., 2014a. Phasic excitation of ventral tegmental dopamine neurons potentiates the initiation of conditioned approach behavior: parametric and reinforcement-schedule analyses. Front. Behav. Neurosci. 8, 155. https://doi.org/10.3389/fnbeh.2014.00155.

Ilango, A., Kesner, A.J., Keller, K.L., Stuber, G.D., Bonci, A., Ikemoto, S., 2014b. Similar roles of substantia nigra and ventral tegmental dopamine neurons in reward and aversion. J. Neurosci. 34 (3), 817–822. https://doi.org/10.1523/JNEUROSCI.1703-13.2014.

Kadar, E., Aldavert-Vera, L., Huguet, G., Costa-Miserachs, D., Morgado-Bernal, I., Segura-Torres, P., 2011. Intracranial self-stimulation induces expression of learning and memory-related genes in rat amygdala. Genes Brain Behav. 10 (1), 69–77. https://doi.org/10.1111/j.1601-183X.2010.00609.x.

Klapoetke, N.C., Murata, Y., Kim, S.S., Pulver, S.R., Birdsey-Benson, A., Cho, Y.K., et al., 2014. Independent optical excitation of distinct neural populations. Nat. Methods 11 (3), 338–346. https://doi.org/10.1038/nmeth.2836.

Kolodziej, A., Lippert, M., Angenstein, F., Neubert, J., Pethe, A., Grosser, O.S., et al., 2014. SPECT-imaging of activity-dependent changes in regional cerebral blood flow induced by electrical and optogenetic self-stimulation in mice. NeuroImage 103, 171–180. https://doi.org/10.1016/j.neuroimage.2014.09.023.

Lammel, S., Steinberg, E.E., Földy, C., Wall, N.R., Beier, K., Luo, L., Malenka, R.C., 2015. Diversity of transgenic mouse models for selective targeting of midbrain dopamine neurons. Neuron 85 (2), 429–438. https://doi.org/10.1016/j.neuron.2014.12.036.

Langlois, L.D., Nugent, F.S., 2017. Opiates and Plasticity in the ventral tegmental area. ACS Chem. Neurosci. https://doi.org/10.1021/acschemneuro.7b00281.

Lin, J.Y., 2011. A user's guide to channelrhodopsin variants: features, limitations and future developments. Exp. Physiol. 96 (1), 19–25. https://doi.org/10.1113/expphysiol.2009.051961.

Lohani, S., Poplawsky, A.J., Kim, S.-G., Moghaddam, B., 2017. Unexpected global impact of VTA dopamine neuron activation as measured by opto-fMRI. Mol. Psychiatry 22 (4), 585–594. https://doi.org/10.1038/mp.2016.102.

Lou, Y., Luo, W., Zhang, G., Tao, C., Chen, P., Zhou, Y., Xiong, Y., 2014. Ventral tegmental area activation promotes firing precision and strength through circuit inhibition in the primary auditory cortex. Front. Neural Circuits 8, 25. https://doi.org/10.3389/fncir.2014.00025.

Morales, M., Margolis, E.B., 2017. Ventral tegmental area: cellular heterogeneity, connectivity and behaviour. Nat. Rev. Neurosci. 18 (2), 73–85. https://doi.org/10.1038/nrn.2016.165.

Mylius, J., Happel, M.F.K., Gorkin, A.G., Huang, Y., Scheich, H., Brosch, M., 2015. Fast transmission from the dopaminergic ventral midbrain to the sensory cortex of awake primates. Brain Struct. Funct. 220 (6), 3273–3294. https://doi.org/10.1007/s00429-014-0855-0.

Negus, S.S., Miller, L.L., 2014. Intracranial self-stimulation to evaluate abuse potential of drugs. Pharmacol. Rev. 66 (3), 869–917. https://doi.org/10.1124/pr.112.007419.

Olds, J., Milner, P., 1954. Positive reinforcement produced by electrical stimulation of septal area and other regions of rat brain. J. Comp. Physiol. Psychol. 47 (6), 419–427.

Olds, M.E., Olds, J., 1969. Effects of lesions in medial forebrain bundle on self-stimulation behavior. Am. J. Physiol. 217 (5), 1253–1264.

Ranaldi, R., Ferguson, S., Beninger, R.J., 1994. Automating the generation and collection of rate-frequency functions in a curve-shift brain stimulation reward paradigm. J. Neurosci. Methods 53 (2), 163–172.

Ranck, J.B., 1975. Which elements are excited in electrical stimulation of mammalian central nervous system: a review. Brain Res. 98 (3), 417–440.

Reichenbach, N., Herrmann, U., Kähne, T., Schicknick, H., Pielot, R., Naumann, M., et al., 2015. Differential effects of dopamine signalling on long-term memory formation and consolidation in rodent brain. Proteome Sci. 13 (1), 13. https://doi.org/10.1186/s12953-015-0069-2.

Rescorla, R.A., Wagner, A.R., 1972. A theory of Pavlovian conditioning: variation in the effectiveness of reinforcement and non reinforcement. In: Black, A.H., Prokasy, W.F. (Eds.), Classical Conditioning (II): Current Research and Theory. Appleton Century Crofts, New York, pp. 64–99.

Schicknick, H., Schott, B.H., Budinger, E., Smalla, K.-H., Riedel, A., Seidenbecher, C.I., et al., 2008. Dopaminergic modulation of auditory cortex-dependent memory consolidation through mTOR. Cereb. Cortex 18 (11), 2646–2658. https://doi.org/10.1093/cercor/bhn026.

Schultz, W., 2017. Reward prediction error. Curr. Biol. 27 (10), R369–R371. https://doi.org/10.1016/j.cub.2017.02.064.

Shumake, J., Ilango, A., Scheich, H., Wetzel, W., Ohl, F.W., 2010. Differential neuromodulation of acquisition and retrieval of avoidance learning by the lateral habenula and ventral tegmental area. J. Neurosci. 30 (17), 5876–5883. https://doi.org/10.1523/JNEUROSCI.3604-09.2010.

Singer, B.F., Bryan, M.A., Popov, P., Robinson, T.E., Aragona, B.J., 2017. Rapid induction of dopamine sensitization in the nucleus accumbens shell induced by a single injection of cocaine. Behav. Brain Res. 324, 66–70. https://doi.org/10.1016/j.bbr.2017.02.018.

Stark, H., Scheich, H., 1997. Dopaminergic and serotonergic neurotransmission systems are differentially involved in auditory cortex learning: a long-term microdialysis study of metabolites. J. Neurochem. 68 (2), 691–697.

Steinberg, E.E., Keiflin, R., Boivin, J.R., Witten, I.B., Deisseroth, K., Janak, P.H., 2013. A causal link between prediction errors, dopamine neurons and learning. Nat. Neurosci. 16 (7), 966–973. https://doi.org/10.1038/nn.3413.

Stuber, G.D., Wise, R.A., 2016. Lateral hypothalamic circuits for feeding and reward. Nat. Neurosci. 19 (2), 198–205. https://doi.org/10.1038/nn.4220.

Takagi, H., Shiosaka, S., Tohyama, M., Senba, E., Sakanaka, M., 1980. Ascending components of the medial forebrain bundle from the lower brain stem in the rat, with special reference to raphe and catecholamine cell groups. A study by the HRP method. Brain Res. 193 (2), 315–337.

Tervo, D.G.R., Hwang, B.-Y., Viswanathan, S., Gaj, T., Lavzin, M., Ritola, K.D., et al., 2016. A Designer AAV variant permits efficient retrograde access to projection neurons. Neuron 92 (2), 372–382. https://doi.org/10.1016/j.neuron.2016.09.021.

Thomsen, S., 1991. Pathologic analysis of photothermal and photomechanical effects of laser-tissue interactions. Photochem. Photobiol. 53 (6), 825–835.

Trulson, M.E., Trulson, T.J., 1987. Recording of mouse ventral tegmental area dopamine-containing neurons. Exp. Neurol. 96 (1), 68–81.

Tsai, H.-C., Zhang, F., Adamantidis, A., Stuber, G.D., Bonci, A., de Lecea, L., Deisseroth, K., 2009. Phasic firing in dopaminergic neurons is sufficient for behavioral conditioning. Science 324 (5930), 1080–1084. https://doi.org/10.1126/science.1168878.

Tye, K.M., Deisseroth, K., 2012. Optogenetic investigation of neural circuits underlying brain disease in animal models. Nat. Rev. Neurosci. 13 (4), 251–266. https://doi.org/10.1038/nrn3171.

Vlachou, S., Markou, A., 2011. Intracranial self-stimulation. In: Olmstead, M.C. (Ed.), Animal Models of Drug Addiction. Humana Press, pp. 3–56. https://doi.org/10.1007/978-1-60761-934-5_1.

Witten, I.B., Steinberg, E.E., Lee, S.Y., Davidson, T.J., Zalocusky, K.A., Brodsky, M., et al., 2011. Recombinase-driver rat lines: tools, techniques, and optogenetic application to dopamine-mediated reinforcement. Neuron 72 (5), 721–733. https://doi.org/10.1016/j.neuron.2011.10.028.

Yizhar, O., Fenno, L.E., Davidson, T.J., Mogri, M., Deisseroth, K., 2011. Optogenetics in neural systems. Neuron 71 (1), 9–34. https://doi.org/10.1016/j.neuron.2011.06.004.

Yona, G., Meitav, N., Kahn, I., Shoham, S., 2016. Realistic numerical and analytical modeling of light scattering in brain tissue for optogenetic applications. eNeuro. https://doi.org/10.1523/ENEURO.0059-15.2015.

Zhang, F., Gradinaru, V., Adamantidis, A.R., Durand, R., Airan, R.D., de Lecea, L., Deisseroth, K., 2010. Optogenetic interrogation of neural circuits: technology for probing mammalian brain structures. Nat. Protoc. 5 (3), 439–456. https://doi.org/10.1038/nprot.2009.226.